



Oilseed-based metabolic engineering of astaxanthin and related ketocarotenoids using a plant-derived pathway: Lab-to-field-to-application

Hyojin Kim¹, Lingyi Liu², Lihua Han³, Kiyoul Park¹, Hae Jin Kim¹, Tam Nguyen¹, Tara J. Nazarene¹, Rebecca E. Cahoon¹, Richard P. Haslam³, Ozan Ciftci^{2,4}, Johnathan A. Napier³  and Edgar B. Cahoon^{1,*} 

¹Center for Plant Science Innovation and Department of Biochemistry, University of Nebraska-Lincoln, Lincoln, NE, USA

²Department of Food Science and Technology, University of Nebraska-Lincoln, Lincoln, NE, USA

³Plant Sciences Department, Rothamsted Research, Harpenden, UK

⁴Department of Biological Systems Engineering, University of Nebraska-Lincoln, Lincoln, NE, USA

Received 7 February 2025;

revised 19 April 2025;

accepted 12 May 2025.

*Correspondence (Tel +1 402-875-0552; fax +1 402-472-3139; email ecahoon2@unl.edu)

Summary

Ketocarotenoids, including astaxanthin, are red lipophilic pigments derived from the oxygenation of β -carotene ionone rings. These carotenoids have exceptional antioxidant capacity and high commercial value as natural pigments, especially for aquaculture feedstocks to confer red flesh colour to salmon and shrimp. Ketocarotenoid biosynthetic pathways occur only in selected bacterial, algal, fungal and plant species, which provide genetic resources for biotechnological ketocarotenoid production. Toward pathway optimization, we developed a transient platform for ketocarotenoid production using *Agrobacterium* infiltration of *Nicotiana benthamiana* leaves with plant (*Adonis aestivalis*) genes, carotenoid β -ring 4-dehydrogenase 2 (CBFD2) and carotenoid 4-hydroxy- β -ring 4-dehydrogenase (HBFD1), or bacterial (*Brevundimonas*) genes, β -carotene ketolase (crtW) and β -carotene hydroxylase (crtZ). In this test system, heterologous expression of the plant-derived astaxanthin pathway conferred higher astaxanthin production with fewer ketocarotenoid intermediates than the bacterial pathway. We evaluated the plant-derived pathway for ketocarotenoid production using the oilseed camelina (*Camelina sativa*) as a production platform. Genes for CBFD2 and HBFD1 and maize phytoene synthase were introduced under the control of seed-specific promoters. In contrast to prior research with bacterial pathways, our strategy resulted in nearly complete conversion of β -carotene to ketocarotenoids, including primarily astaxanthin. Tentative identities of other ketocarotenoids were established by chemical evaluation. Seeds from multi-season US and UK field sites maximally accumulated ~135 $\mu\text{g/g}$ seed weight of ketocarotenoids, including astaxanthin (~47 $\mu\text{g/g}$ seed weight). Although plants had no observable growth reduction, seed size and oil content were reduced in astaxanthin-producing lines. Oil extracted from ketocarotenoid-accumulating seeds showed significantly enhanced oxidative stability and was useful for food oleogel applications.

Keywords: aquaculture, antioxidant, β -carotene ketolase, β -carotene hydroxylase, camelina.

Introduction

Ketocarotenoids, including astaxanthin (3,3'-dihydroxy- β , β' -carotene-4,4'-dione), are distinguished by the presence of a carbonyl or keto group on one or both carotenoid ionone rings (Maoka, 2020). Unlike other carotenoids that have a yellow or orange hue, astaxanthin exhibits a bright red colour resulting from additional conjugated double bonds in the keto groups on its ionone rings (Meléndez-Martínez *et al.*, 2007). A number of fish and crustaceans that are obtained from rivers and oceans and from aquaculture, including salmon, trout and shrimp, accumulate dietary astaxanthin, resulting in the distinctive red colour of their flesh (Maoka, 2020). While aquaculture is considered a more sustainable food production system compared to conventional fishing, this industry has a high demand for astaxanthin as a feed

component (Elbahnaswy and Elshopakey, 2024). This demand arises from consumer desire for the bright red colour of selected farmed fish (e.g. salmon and trout) and crustaceans (e.g. shrimp and krill). Industrial demand has also increased for the use of astaxanthin as a natural food colouring application (Nakano, 2020). In addition to its colour, astaxanthin has gained increasing interest for use in nutraceutical and cosmetic products due to its potent antioxidant and photoprotective properties (O'Connor and O'Brien, 1998; Santocono *et al.*, 2006; Saganuma *et al.*, 2010). Astaxanthin has ~10 times more free-radical scavenging activity than other carotenoids, including β -carotene and zeaxanthin, and ~100-times more free-radical scavenging activity than α -tocopherol (Miki, 1991). Additionally, astaxanthin has been shown to suppress ultraviolet A (UVA)-induced oxidative damage to cells, and it is 100 times more effective than

Please cite this article as: Kim, H., Liu, L., Han, L., Park, K., Kim, H.J., Nguyen, T., Nazarene, T.J., Cahoon, R.E., Haslam, R.P., Ciftci, O., Napier, J.A. and Cahoon, E.B. (2025) Oilseed-based metabolic engineering of astaxanthin and related ketocarotenoids using a plant-derived pathway: Lab-to-field-to-application. *Plant Biotechnol. J.*, <https://doi.org/10.1111/pbi.70148>.

β -carotene in protecting against UVA-induced oxidative stress using in vitro (O'Connor and O'Brien, 1998; Santocono et al., 2006; Sukanuma et al., 2010). Collectively, the demand for astaxanthin production, particularly for use in aquaculture, nutraceuticals, cosmetics and functional foods, is rapidly expanding due to its potent antioxidant activity and distinctive pigmentation (Debnath et al., 2024). Global market forecasts estimate the industry will exceed USD 1.9 billion by 2025 and reach over USD 2.2 billion by 2027 (Grand View Research, 2024). Astaxanthin is synthesized by modification of the ionone rings of β -carotene. Divergent astaxanthin biosynthetic pathways are found in selected bacteria (e.g. *Brevundimonas* sp. *Paracoccus carotinifaciens*), yeast (e.g. *Xanthophyllomyces dendrorhous*) and green algae (e.g. *Haematococcus pluvialis*) (Elbahnaswy and Elshopakey, 2024). Astaxanthin biosynthesis also has limited occurrence in flowering plants, most notably in the flower petals of *Adonis* species (Renström et al., 1981; Seybold and Goodwin, 1959). Commercially produced 'natural' astaxanthin is largely extracted from the green alga *Haematococcus pluvialis* and the basidiomycetous yeast *X. dendrorhous* (formerly *Phaffia rhodozyma*). Bacteria such as *Brevundimonas* sp. produce astaxanthin naturally at <0.03% of their dry weight, microalgae including *H. pluvialis* can accumulate astaxanthin to <5% of their dry weight under stress conditions and yeast *X. dendrorhous* typically accumulates astaxanthin to <1% of its dry weight. Flowering plants, such as *Adonis amurensis* and *A. aestivalis*, accumulate esterified astaxanthin to <1.3% of their dry weight in flower petals (Li et al., 2021; Maoka et al., 2011).

These organisms use distinct enzymes and metabolic pathways for astaxanthin biosynthesis. Marine bacteria and microalgae, for example, use crtW (synonymous with BKT) and crtO as β -carotene ketolases and crtZ (synonymous with crtR-b or chy) as β -carotene hydroxylases (Álvarez et al., 2006; Fernández-González et al., 1997; Ojima et al., 2006; Ukibe et al., 2009). In the yeast *X. dendrorhous*, a specialized astaxanthin synthase and cytochrome P450 module (crtS-crtR) catalyses all steps from β -carotene to ketocarotenoid including astaxanthin (Alcaíno et al., 2012; Álvarez et al., 2006; Ojima et al., 2006; Ukibe et al., 2009). Astaxanthin biosynthesis in *A. aestivalis* flower petals occurs in plastids and involves coordinated reactions catalysed by carotenoid β -ring 4-dehydrogenase enzymes (CBFD1 and CBFD2) and carotenoid 4-hydroxy- β -ring 4-dehydrogenase enzymes (HBFD1 and HBFD2) to introduce the 3, 3' hydroxyl and 4, 4' keto groups on the β -carotene ionone rings (Cunningham Jr and Gantt, 2011).

Genes encoding these enzymes, particularly those from microbial sources, have been used extensively for plant metabolic engineering for the production of astaxanthin and other ketocarotenoids (e.g. Farré et al., 2016; Fujisawa et al., 2009; Ha et al., 2019; He et al., 2022; Liu et al., 2021; Lu et al., 2017; Park et al., 2017; Wang et al., 2021; Zhu et al., 2018). The use of transgenes encoding combinations of microbial enzymes resulted in both astaxanthin biosynthesis and the accumulation of intermediates, including adonixanthin, adonirubin, canthaxanthin and echinenone. For example, engineered rapeseed expressing a combination of crtW and crtZ from marine bacterium or a combination of microalgal BKT and CHY produced carotenoid biosynthetic intermediates at levels that were 300-fold or fourfold higher than that of astaxanthin, respectively (Fujisawa et al., 2009; Wang et al., 2021). In another study, tomato engineered to express microalgal BKT and BHY accumulated ketocarotenoid intermediates at levels comparable to those of

astaxanthin (Huang et al., 2013). Recent studies have also used transgenes to express the *Adonis* biosynthetic enzymes (Allen et al., 2022; Liu et al., 2021). The introduction of these transgenes into *Nicotiana benthamiana* resulted in partial conversion of β -carotene into astaxanthin (Allen et al., 2022). Liu et al. (2021) successfully generated transgenic maize plants using the *Adonis* biosynthetic genes, which yielded 49 mg/kg DW of astaxanthin. In contrast, their attempt to combine microbial and *Adonis* biosynthetic modules did not result in plant regeneration from transformed calli.

In this report, we explored the use of the Brassicaceae oilseed crop camelina (*Camelina sativa* L.) as an astaxanthin production platform. In addition to its agronomic attributes, including productivity with minimal water and fertility inputs, camelina is an ideal crop for metabolic engineering and synthetic biology studies (Iskandarov et al., 2014). This crop can be readily transformed with a simple, low-labour input *Agrobacterium tumefaciens* floral infiltration and has a relatively short life cycle (90–120 days) (Iskandarov et al., 2014). Camelina's utility for metabolic engineering has been demonstrated for a number of different specialty industrial and edible oil applications and biopolymer production (e.g. Konda et al., 2023; Malik et al., 2018; Xi et al., 2016; Yuan and Li, 2020), including a recent report for astaxanthin production using microbial genes (He et al., 2022). It has also been shown that engineered camelina can be field grown to obtain sufficient amounts of seeds for downstream evaluation of traits in food, feed and industrial applications (Napier and Betancor, 2023; Napier and Sayanova, 2020; Yuan and Li, 2020). In this report, we initially compared metabolic engineering strategies for bacterial (*Brevundimonas* sp.) and plant (*A. aestivalis*) astaxanthin biosynthetic pathways using transient gene expression in *N. benthamiana*. Based on these results, we employed seed-specific expression of *A. aestivalis* astaxanthin biosynthetic genes along with a maize phytoene synthase gene to enhance β -carotene substrate levels. We describe the field performance of these lines over two seasons in two geographic locations and the use of ketocarotenoid-rich oils extracted from seeds of these lines for novel food science applications.

Results

Evaluation of astaxanthin biosynthetic genes via transient expression assays

To develop a metabolic engineering strategy for oilseed astaxanthin production, we first assessed biosynthetic genes from the bacterium *Brevundimonas* sp. and the plant *A. aestivalis* (Figure S1). We synthesized genes for bacterial crtW and crtZ, and plant HBFD1 and CBFD2 that were codon-optimized for *Arabidopsis thaliana*. For crtW and crtZ, we also included coding sequences for an N-terminal plastid transit peptide from the *Arabidopsis* RuBISCO small subunit (Figure 1). The synthetic genes were assembled into binary vectors flanked by the constitutive CaMV35S promoter and 3' UTR, and used for transient assays in *N. benthamiana* leaves. In these assays, the expressed enzymes utilized the endogenous chloroplast pool of β -carotene to convert it into astaxanthin and other ketocarotenoids. The *Adonis* gene set (CBFD2 and HBFD1, or 'ASTA') and bacterial gene set (crtW and crtZ, or 'crtWZ') were transiently introduced into *N. benthamiana* leaves via infiltration of *A. tumefaciens* harbouring binary vectors (Figure 1). Expression of the transgenes led to the visible accumulation of red/orange ketocarotenoid pigments

in *N. benthamiana* leaves. Five days after infiltration (DAI), total carotenoids extracted from the leaves were analysed using thin layer chromatography (TLC) and high-performance liquid chromatography with diode array detection (HPLC-DAD) (Figure 2 and Table S1).

From TLC analysis, we observed two strong yellow bands in the control leaf and six orange-red ketocarotenoids and two yellow bands in the ASTA and crtWZ lanes (Figure 2). In the control leaves, lutein accounted for 68%, and β -carotene for 32% of the

total carotenoids, with no detectable ketocarotenoids based on HPLC measurements. In contrast, leaves infiltrated with ASTA and crtWZ produced carotenoids found in control leaves as well as ketocarotenoids, including astaxanthin, which comprised up to 44% of total carotenoids (Table S1). TLC analysis of ASTA-infiltrated leaves revealed a bright red astaxanthin band (based on mobility relative to an authentic standard) and faint orange/red bands corresponding to an unknown ketocarotenoid as well as adonixanthin, adonirubin, canthaxanthin and echinenone. In

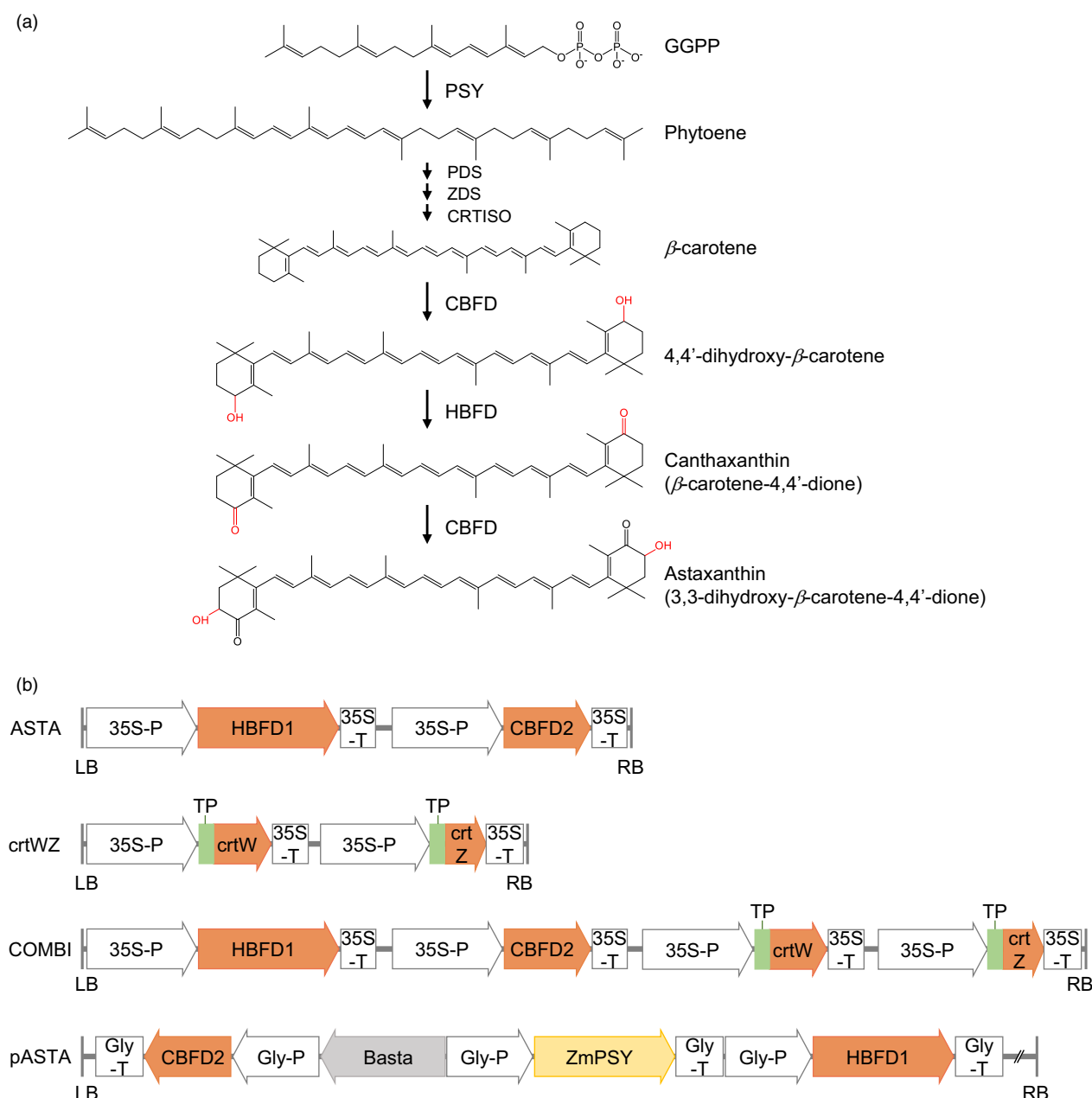


Figure 1 Astaxanthin biosynthesis pathway identified in *Adonis aestivalis* (a) and schematic diagram of the T-DNA region of the binary vectors, ASTA, crtWZ, COMBI and pASTA, used in the study (b). 35S-P, Cauliflower Mosaic Virus 35S promoter; 35S-T, Cauliflower Mosaic Virus 35S terminator; CBFD2, carotenoid β -ring 4-dehydrogenase (Genbank: AY644758.1); crtW, β -carotene ketolase (Genbank: QVQ68840.1); crtZ, β -carotene hydroxylase (Genbank: WP_183216731.1); GGPP, geranylgeranyl pyrophosphate; Gly-P, glycinin promoter; Gly-T, glycinin terminator; HBFD1, carotenoid 4-hydroxy- β -ring 4-dehydrogenase (Genbank: DQ902555.1); PSY, phytoene synthase; TP, transit peptide for small subunit of Rubisco complex; ZmPSY, PSY gene from *Zea mays* (Genbank: NM_001114652.2). The *Basta* gene encodes phosphinothricin N-acetyltransferase, which provides resistance to herbicide applications. *Adonis*-specific enzymatic reactions are shown in red.

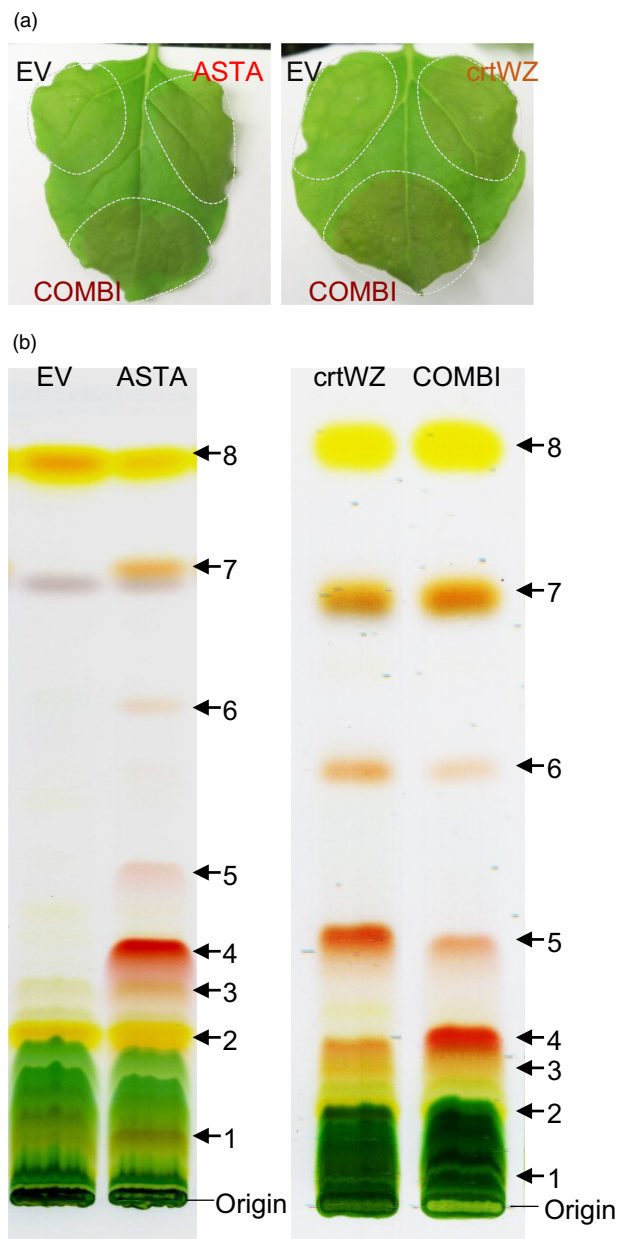


Figure 2 TLC analysis of *Nicotiana benthamiana* leaves transiently expressing *Adonis* genes or bacterial genes involved in astaxanthin biosynthesis. (a) Images of *N. benthamiana* leaves transiently expressing astaxanthin biosynthetic genes. (b) The carotenoids were extracted using a mixture of methanol and dichloroform (75:25, v/v) then separated on a TLC plate with mobile phase toluene:acetone (80:20, v/v). 1, Ketocarotenoid (unknown). 2, Lutein. 3, Adonixanthin. 4, Astaxanthin. 5, Adonirubin/phoenicoxanthin. 6, Canthaxanthin. 7, Echinenone. 8, β -carotene.

contrast, ketocarotenoids detected in *crtWZ*-infiltrated leaves were principally adonirubin, with lesser amounts of astaxanthin, canthaxanthin, echinenone and adonixanthin (Figure 2). HPLC quantification showed that astaxanthin constituted ~55% of total ketocarotenoids in *ASTA*-infiltrated leaves versus ~34% in *crtWZ*-infiltrated leaves (Table S1). This difference appeared to be due to the low efficiency of conversion of adonirubin into astaxanthin by the β -carotene hydroxylase (*crtZ*) enzyme, resulting in the

accumulation of ketocarotenoid intermediates (e.g. adonirubin and canthaxanthin) in the plant host. Overall, our results suggested that the plant-derived astaxanthin pathway is more efficient than the bacterial-derived pathway for astaxanthin production in a plant host.

We further tested the effect of co-expression of plant- and bacterial-derived astaxanthin pathways on astaxanthin production in *N. benthamiana* leaves. The combination of *Adonis* and bacterial genes, referred to as 'COMBI', was constructed using the Golden-Braid gene stacking method and was *Agrobacterium*-infiltrated (see Experimental procedures; Figures 1b and 2). The ketocarotenoids produced in COMBI-infiltrated leaves accounted for ~52% of total carotenoids, of which ~53% was in the form of astaxanthin (Table S1). Astaxanthin production was improved in COMBI-infiltrated leaves compared to *crtWZ*-infiltrated leaves, but showed little difference from ketocarotenoid and astaxanthin production using *ASTA* alone. The relative amount of adonirubin was only ~9% of total carotenoids, likely resulting from enhanced conversion of adonirubin to astaxanthin by the *CBFD2* enzyme (Table S1). Overall, our results from *N. benthamiana* transient expression suggest that the plant-derived pathway (*Adonis*) may result in higher astaxanthin titers and fewer ketocarotenoid intermediates in the plant host compared to the bacterial pathway, under the conditions tested. However, further investigation would be required to fully assess the comparative efficiency of these pathways.

Oilseed-based production of astaxanthin in camelina

Based on the findings from transient expression in *N. benthamiana*, we pursued a strategy for oilseed metabolic engineering to produce astaxanthin by using the *Adonis CBFD2* and *HBFD1* genes. We used camelina as the oilseed platform, given its relative ease of genetic transformation (Lu and Kang, 2008). Because camelina seeds have relatively low β -carotene concentrations (Kiczorowska et al., 2019), we included a transgene for maize (*Zea mays*) phytoene synthase (*ZmPSY*) to enhance flux in the plastid isoprenoid pathway for β -carotene biosynthesis. A plant binary vector, pASTA, was designed to carry transgenes encoding *CBFD2*, *HBFD1* and *ZmPSY*, all under control of a seed-specific glycinin promoter (Figure 1b). The transgenes from the pASTA vector were introduced via *A. tumefaciens* floral infiltration into camelina. Approximately 20 T₁ red/orange seeds, representing independent events, were visually selected, and 10 independent lines exhibiting a 3:1 segregation ratio were advanced to the next generation (Figure S1a). The two leading lines, exhibiting stable inheritance of introduced genes, accumulated 15–17 $\mu\text{g/g}$ dry weight (DW) of astaxanthin in their seeds (Figure S1b,c). A line with the highest astaxanthin seed concentrations was advanced under greenhouse cultivation to homozygosity. Using RT-PCR analysis, we confirmed the expression of the *CBFD2*, *HBFD1* and *ZmPSY* transgenes in developing astaxanthin-producing camelina (hereafter, designated "pASTA") seeds (Figure S1d). The developing embryo from pASTA initiated production and accumulation of red pigment at ~18 days after flowering (DAF) (Figure 3a). The dry seeds of the pASTA line exhibited a distinct orange-red pigmentation compared to the brown coloration of wild-type seeds (Figure 3b). Although this altered pigmentation had no observable effect on embryogenesis, developing seeds at 25–28 DAF displayed reduced accumulation of chlorophyll *a* and decreased expression of genes associated with chloroplast development (Figure 3b,c and Figure S2). Seed measurements showed that transgenic seeds had a smaller median area

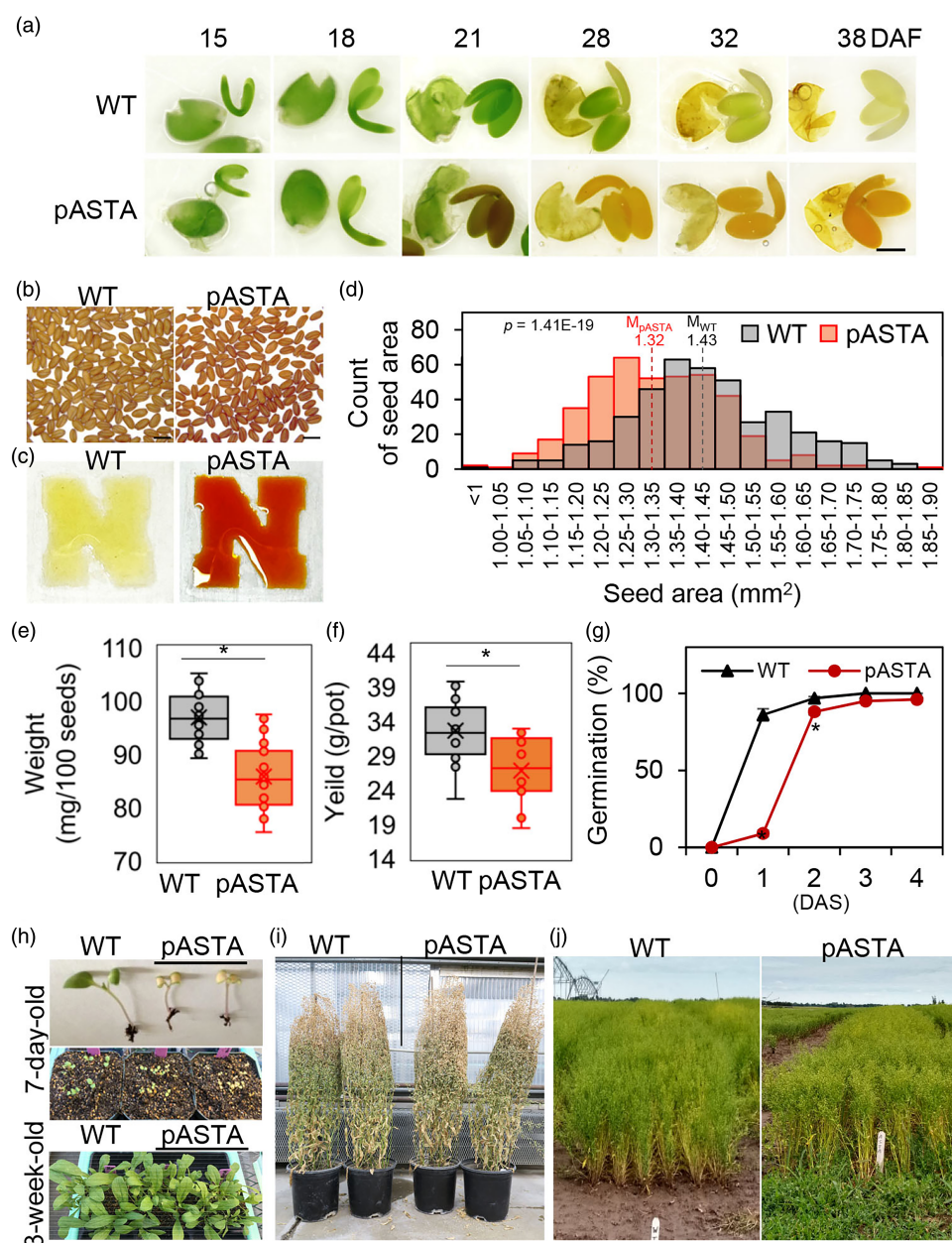


Figure 3 Characterization of seed development, yield and germination from planting to harvest in WT and pASTA. (a) Images of representative cotyledons excised from the seed coat from 15 to 38 days after flowering (DAF). Scale = 1 mm. (b, c) Dry seed and extracted seed oil by a press. Scale = 2 mm. (d) Histogram of seed area. Seed area was measured using digital images of 400 seeds each using ImageJ (<https://imagej.net/ij/>). M_{pASTA} , median value of pASTA. M_{WT} , median value of WT. Student's *t*-test was used to generate the *P* values. n.s., non-significant. (e) Seed weight per 100 seeds. Seed weight was measured in 28 replicates. **P* < 0.001, student's *t*-test. (f) Seed yield per pot from greenhouse. Three plants were grown in each of 16 pots, and seeds were harvested separately from each pot in greenhouse. *, *p* < 0.001, student's *t*-test. (g) Seed germination test. Hundred seeds were tested on the wet paper and the radical appearance was counted. Values are the mean of three replicates ± SD. **P* < 0.001, student's *t*-test. DAS, days after sowing. (h) Seven-day-old and 3-week-old camelina plants growing in the greenhouse. (i) Mature camelina plants observed 5 days before seed harvest, grown in the greenhouse. (j) Camelina growing at the field at ENREC, NE.

(1.32 mm²) and lower average seed weight (85 mg/100 seeds), compared to the wild type (1.43 mm² and 96 mg/100 seeds, respectively), indicating a reduction in both seed size and weight (Figure 3d,e). In addition, seed yield was assessed by measuring the total seed weight harvested from greenhouse-grown plants. The wild-type plants produced an average of 32 g of seeds per

pot, whereas the transgenic line yielded 26 g, indicating a trend toward reduced seed yield in the transgenic plants (Figure 3f). Germination tests revealed that wild-type seeds exhibited approximately 90% germination within 1 day, while transgenic seeds required 2 days to achieve similar germination rates (Figure 3g). After germination, cotyledon development differed

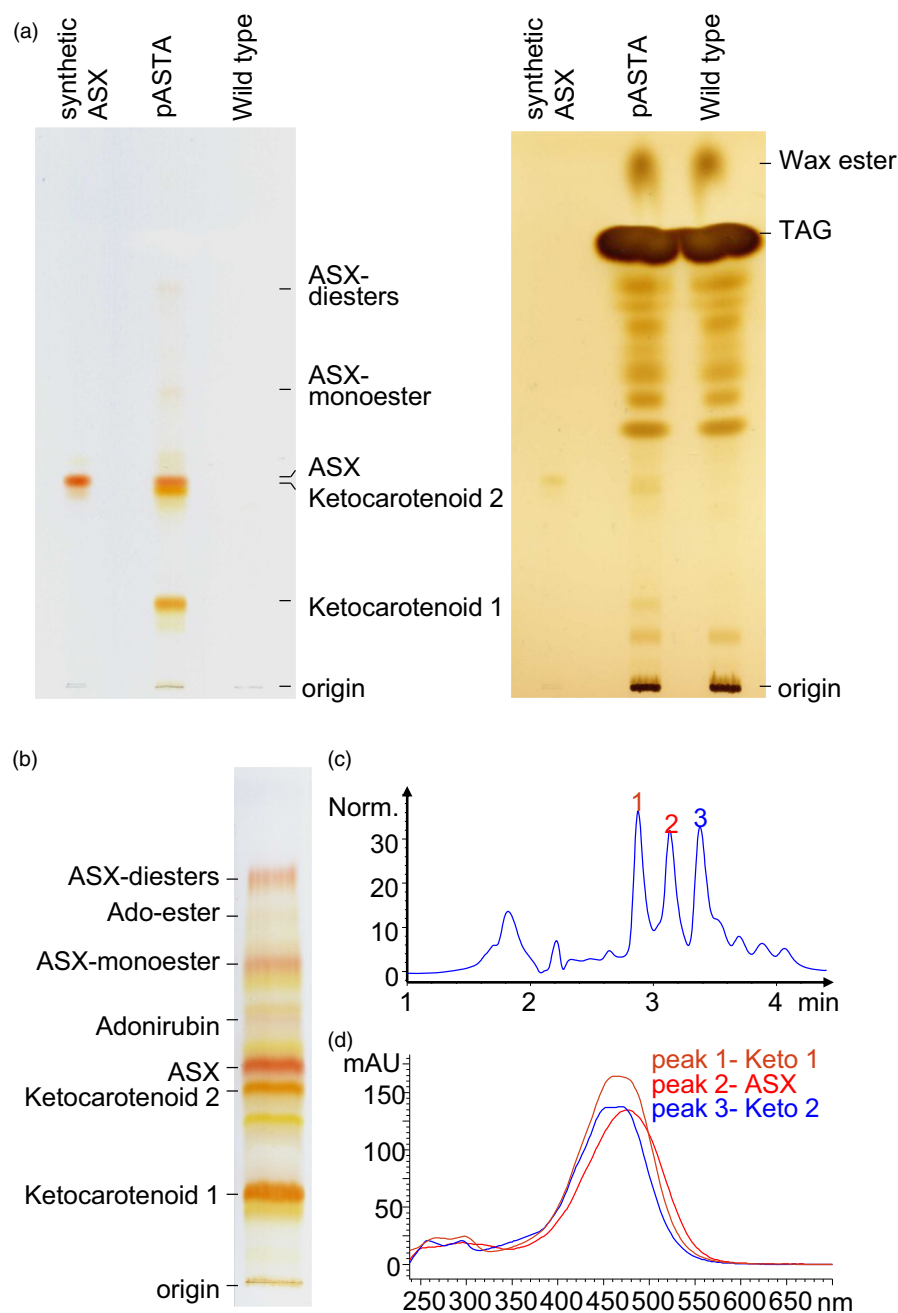


Figure 4 TLC analysis (a and b) and HPLC analysis (c and d) of total carotenoids extracted from pASTA seeds grown in a greenhouse. (a) Separation of carotenoids on TLC plate (left) and iodine-stained TLC image (right). Total extracts from seeds of wild type or pASTA were analysed using TLC. TLC was run using two different mobile phases. The first mobile phase was heptane:ethyl ether:acetic acid (70:30:1, v/v), second mobile phase was toluene:acetone (80:20, v/v). (b) Separation of carotenoids on TLC plate. The neutral lipid (wax esters and triacylglycerol) were separated on the TLC plate with the mobile phase heptane:ethyl ether:acetic acid (70:30:1, v/v). Then the carotenoids were scraped and purified. The extracts with acetone were separated on the TLC plate with the mobile phase toluene:acetone (80:20, v/v). (c) The HPLC chromatogram of ketocarotenoids extracted from pASTA seeds. Peak 1, ketocarotenoid 1; peak 2, astaxanthin; peak 3, ketocarotenoid 2. (d) Absorbance spectrum of ketocarotenoid 1, astaxanthin, and ketocarotenoid 2, which are shown in (c).

between the lines: wild-type seeds developed green cotyledons, while transgenic seeds retained a yellow-bleached coloration (Figure 3h). Although transgenic seedlings showed slower development during the first 3 weeks, no significant developmental differences were observed thereafter, and both lines exhibited similar growth up to the time of seed harvesting (Figure 3h–j).

We initially evaluated ketocarotenoid production in oil extracted from pASTA seeds using TLC. We separated triacylglycerols from carotenoids by TLC using development in two solvent systems with differing polarities (see Experimental procedures; Figure 4a). This revealed not only astaxanthin (based on mobility relative to an authentic standard) but also two prominent red/orange-coloured pigments, designated 'ketocarotenoid 1' and

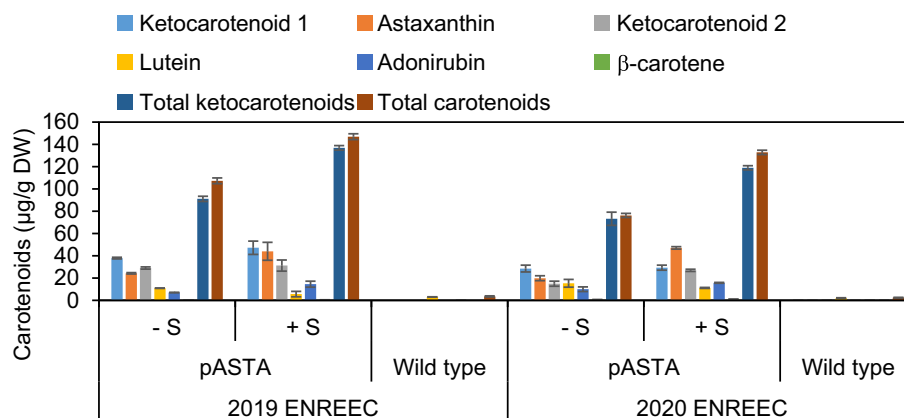


Figure 5 The carotenoids content in seeds of wild type and pASTA grown in the field at ENREEC, NE. Values are means ($\mu\text{g/g DW}$) \pm SD of analysis of three independent samples. –S, without saponification. +S, with saponification.

'ketocarotenoid 2' with lesser mobility on TLC than astaxanthin, suggesting greater polarity than astaxanthin (e.g. more hydroxylation). Small amounts of ketocarotenoid esters (astaxanthin-diester, astaxanthin-monoester, adonirubin-ester) were also detected in pASTA seeds (Figure 4a,b and Figure S4). No red pigments were detected in wild-type seeds. As shown in Figure 4c,d, we detected three ketocarotenoid peaks including astaxanthin with identical absorption spectra from HPLC-DAD. The spectrum of the astaxanthin (peak 2) in methanol and its maximum absorption wavelength of ~ 480 nm was consistent with the known spectrum of astaxanthin. The maximum absorption wavelength of ketocarotenoid 1 (peak 1) was ~ 465 nm. The spectral absorption shape of ketocarotenoid 2 (peak 3) was similar to that of adonixanthin (ketozeaxanthin) or ketolutein, and its maximum absorption wavelengths were ~ 455 nm and ~ 470 nm (Mulders *et al.*, 2015; Yuan and Chen, 2000).

To determine the structures of the two unknown ketocarotenoids (ketocarotenoids 1 and 2), we investigated the presence of ketone and hydroxyl groups on ketocarotenoids by reducing keto groups to hydroxyl groups with sodium borohydride or by modifying hydroxyl groups through trimethylsilylation using N,O-bis(trimethylsilyl)acetamide. For these analyses, we first purified ketocarotenoid 1, ketocarotenoid 2 and astaxanthin individually by TLC from the total carotenoid extract of pASTA seeds. The reduced ketocarotenoids, including astaxanthin, lost their orange-red colour and exhibited decreased TLC mobility, likely due to the lower polarity of the introduced hydroxyl groups (Figure S5a). Reduced astaxanthin generated two bands corresponding to partial and full reduction, consistent with sequential structural modifications to: (1) idoxanthin (3,3',4'-trihydroxy- β , β' -carotene-4-one; orange-red) and (2) crustaxanthin (3,3',4,4'-tetrahydroxy- β -carotene; yellow) (Figure S5a). Based on the number of bands and their TLC mobility, we deduced that ketocarotenoid 1 and 2 each contain one keto group on their β -ionone rings. Additionally, the TMS derivative of astaxanthin showed two expected sequential products from partial and full reaction: (1) the mono-TMS derivative and (2) the di-TMS derivative (Figure S5b). The TMS reaction of ketocarotenoid 1 yielded one primary product from complete trimethyl silylation and additional bands from partial reaction, whose number and position are most consistent with the three hydroxyl groups and their positions found on idoxanthin (Figure S5c,d). The TMS

reaction of ketocarotenoid 2 produced a primary product from complete trimethylsilylation, along with two products from partial reactions, consistent with the presence of two hydroxyl groups on the β -ionone rings, similar to the structures of ketolutein and adonixanthin.

Field evaluation of astaxanthin-producing camelina lines

The top astaxanthin-producing camelina line pASTA from greenhouse-based studies was evaluated in dedicated biotech fields located in two distinct geographical locations: the Eastern Nebraska Research, Extension, and Education Center (ENREEC) in Mead, Nebraska, USA (2019 and 2020 growing seasons), and Rothamsted Research (RRes) in Harpenden, Hertfordshire, UK (2016–2018 and 2020 growing seasons). Wild-type and pASTA seeds were harvested from field plots and evaluated for seed traits, including ketocarotenoids, tocopherols and seed oil content. Seeds harvested from the US site were also used for oil extraction and subsequent food science applications (see below).

The ketocarotenoids in the seeds of wild type and pASTA grown in the field at ENREEC in 2019 and 2020 growing seasons were analysed by HPLC-DAD (Figure 5). Total extracts were saponified by adding sodium hydroxide to accurately quantify the ketocarotenoids due to the ketocarotenoid fatty acid esters in pASTA seeds. According to quantitative analysis, total carotenoids in pASTA seeds were approximately 50-fold higher than in wild-type seeds. The ketocarotenoids accumulated in pASTA seeds accounted for >90% of total carotenoids. Of this amount, astaxanthin accounted for 48% (in 2019) and 40% (in 2020) of the total ketocarotenoids. Total ketocarotenoid concentrations were 122 $\mu\text{g/g DW}$ in 2019 and 103 $\mu\text{g/g DW}$ in 2020, and free astaxanthin concentrations were 44 $\mu\text{g/g DW}$ in 2019 and 47 $\mu\text{g/g DW}$ in 2020 after saponification. Based on quantitative analysis, ketocarotenoid esters represented approximately 38% of total ketocarotenoid. The major free or unesterified ketocarotenoid was astaxanthin, followed by adonirubin, in extracts of pASTA seeds. Though astaxanthin was the major ketocarotenoid in pASTA seeds, ketocarotenoid intermediates such as two unknown ketocarotenoids and adonirubin were detected at relative amounts of 60% (in 2020) to 68% (in 2019) of the total ketocarotenoids. In the 2018 and 2020 seasons in the UK RRes field site, total concentrations of free ketocarotenoids including

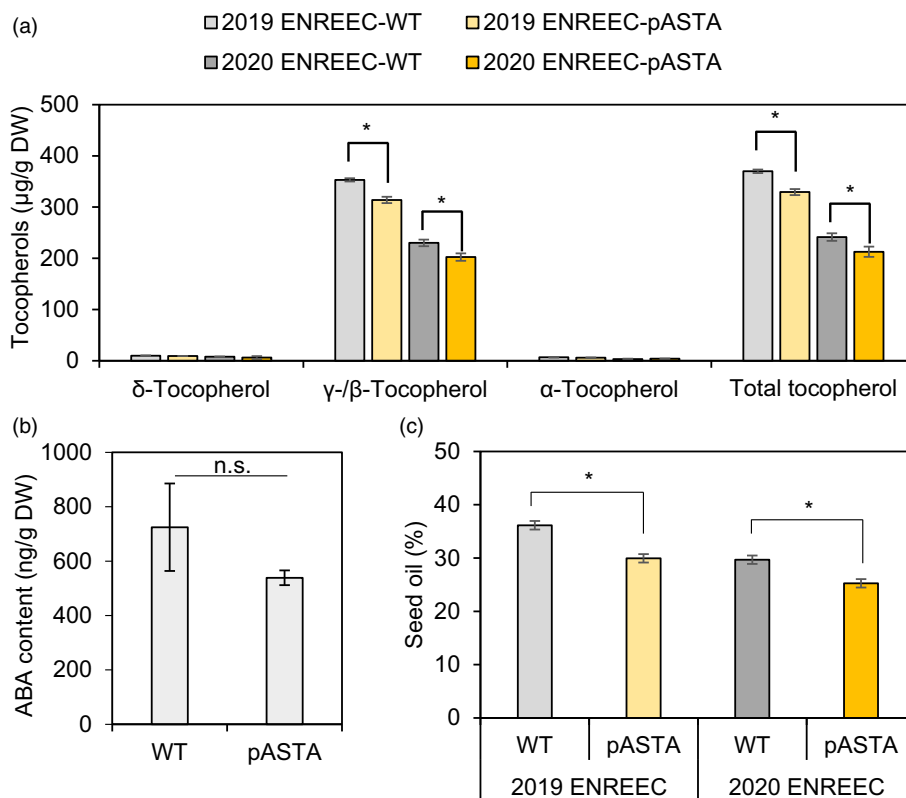


Figure 6 Tocopherol (a), ABA (b) and oil (c) concentrations of seeds from wild type and pASTA grown in the field at Eastern Nebraska Research, Extension and Education Center (ENREEC). Values are means \pm SD of analysis of three independent samples. Student's *t*-test was compared to wild type. **P* < 0.01. n.s., not significant.

two unknown ketocarotenoids and astaxanthin were 44.3 $\mu\text{g/g}$ DW in 2018 and 49.0 $\mu\text{g/g}$ DW in 2020 after saponification (Figure S6a). The proportion of astaxanthin in total ketocarotenoids was 33% in 2018 and 30% in 2020, similar to relative amounts in seeds of US-grown pASTA.

To examine the effects of ketocarotenoid production on pathways that directly compete for biosynthetic precursors, we investigated the level of tocopherols and abscisic acid (ABA). These metabolites were selected as representative markers of two biosynthetic pathways branched from the plastid methylerythritol phosphate (MEP) pathway to examine the effect of altered carotenoid flux. The concentrations of total tocopherols in the seeds of pASTA were 329 $\mu\text{g/g}$ DW in 2019 and 213 $\mu\text{g/g}$ DW in 2020, approximately 88% of wild-type concentrations in both growing seasons (370 $\mu\text{g/g}$ DW in 2019 and 241 $\mu\text{g/g}$ DW in 2020) (Figure 6a). The major form of tocopherols, γ -tocopherol (plus β -tocopherol), was reduced, while α - and δ -tocopherol levels remained unchanged. The ABA levels in seeds of pASTA showed no significant difference compared to wild type (Figure 6b). These results suggest that the introduction of the plant-derived astaxanthin biosynthetic pathway led to the accumulation of ketocarotenoids, with a decrease in tocopherol (from geranylgeranyl diphosphate) and no detectable effect on ABA (from β -carotene) levels in seeds of field-grown lines.

The effects of ketocarotenoid production on seed oil composition and concentration in seeds of wild-type and pASTA lines at the USA and UK field sites were also examined (Figure 6c and Figure S6b,c). The most significant differences in seed oil composition between the two lines were an increase in stearic

acid (18:0) and an alteration in the relative amounts of linolenic acid, which is a fatty acid that responds sensitively to changes in the surrounding environment, such as temperature, in the pASTA seeds compared to the wild-type seeds (Table S2 and Figure S6b). Additionally, the total seed oil content in wild-type seed ranged from 30% to 40% of dry weight depending on the growth location/environment. Total oil content in pASTA seeds was reduced by ~15% in the pASTA lines (Figure 6c and Figure S6c), but no significant differences in triacylglycerol species were detected between wild-type and pASTA seeds (Figure S6d). Total seed nitrogen levels (as a percentage of total dry matter) were slightly elevated in the pASTA seeds, whereas the total seed carbon content showed a slight reduction (Figure S6c). Importantly, in the 2021 UK field trial, pASTA produced seed yields comparable to wild-type controls (Table S3), indicating that astaxanthin production did not negatively impact agronomic performance under these conditions.

Application of astaxanthin oils for food industry as an alternative to solid fats

To assess the potential of pASTA seed oil for food product applications, we examined the effects of its ketocarotenoids on the stability of camelina oil and oleogels. Oleogels are an emerging formulation for generating 'healthy' semi-solid fats for food applications (Martins *et al.*, 2020; Puşcaş *et al.*, 2020). In this study, we generated oleogels by mixing sorghum grain waxes (Liu *et al.*, 2020) with camelina oil pressed from either non-engineered seeds or pASTA seeds (Figure 7a). We used these mixtures to evaluate the oxidative stability of oils and

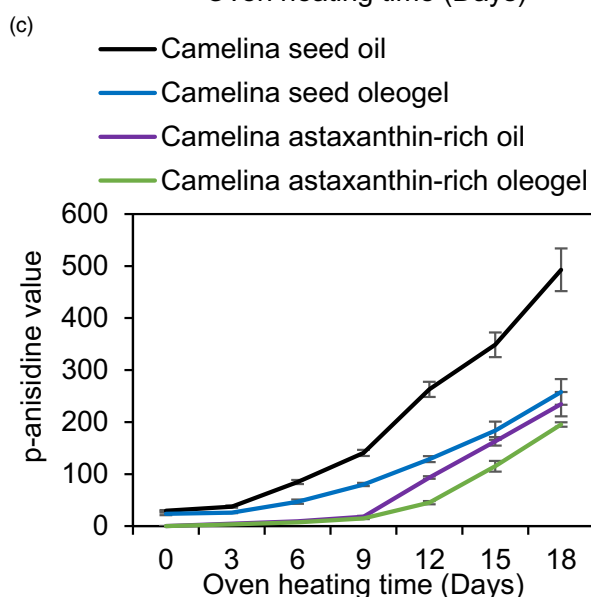
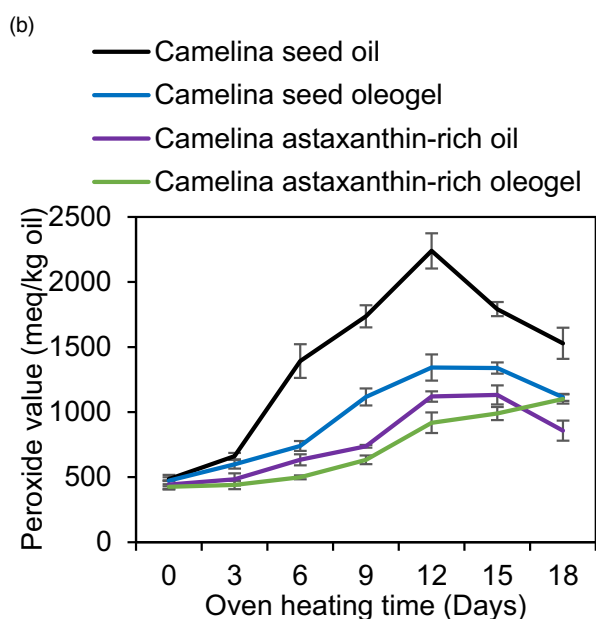
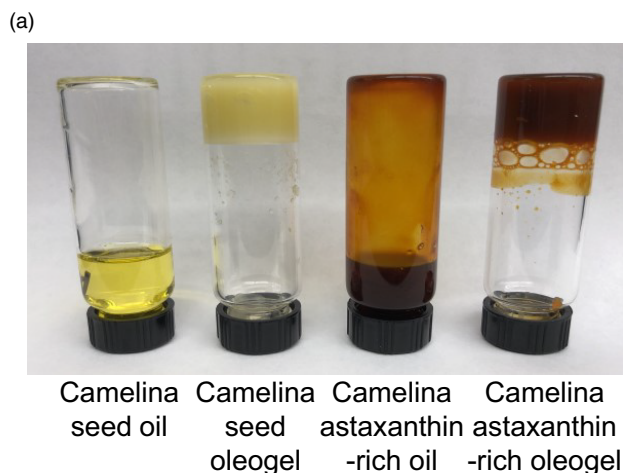


Figure 7 Evaluation of the oxidative stability of oils and oleogels from pressed seed oil of wild-type and pASTA plants grown in the field at ENREEC, NE. (a) Formation of oleogels by mixing sorghum grain waxes with camelina oil pressed from either non-engineered seeds or pASTA seeds. (b) Peroxide values (PV) for primary oxidation products. (c) *p*-anisidine values for secondary products.

oleogels under accelerated storage conditions at 40 °C for up to 18 days. This parameter is of primary importance for the shelf-life of food products prepared using vegetable oils or oleogels. Figure 7 shows the formation of primary and secondary oxidation products in camelina seed oil and its oleogels over the 18-day treatment. Lipid oxidation generally follows a free-radical chain reaction, where hydroperoxides formed from unsaturated fatty acids decompose into secondary oxidation products (Frankel, 1984). To assess oxidative stability, both peroxide values (PV) for primary oxidation products (hydroperoxides) and *p*-anisidine values for secondary products (e.g. aldehydes, ketones, alcohols) were measured. Although the Oxidative Stability Index (OSI), typically measured using a Rancimat instrument and commonly used in the industry, offers a single-value indicator under accelerated conditions, PV and *p*-anisidine values allow more detailed tracking of oxidation stages. Therefore, their combined use offers a comprehensive alternative to OSI in evaluating oxidative stability. Figure 7b showed, in the first 3 days, camelina seed oil had the highest PV increase, while the PV of astaxanthin-rich camelina seed oil oleogels showed minimal change. After Day 3, PV rose sharply in camelina seed oil but more gradually in the other samples. By Day 12, all samples reached peak PV, with astaxanthin-rich camelina seed oil oleogel showing the lowest PV. The PV decline after Day 12, except in astaxanthin-rich oleogels, is due to hydroperoxides breaking down into secondary products that cause rancidity. This rancidity developed earlier in regular camelina seed oil, indicating lower oxidative stability compared to astaxanthin-rich oils.

A similar trend was observed for *p*-anisidine values, with camelina seed oil showing the highest value, followed by camelina seed oleogel, astaxanthin-rich camelina oil and its oleogel form (Figure 7c). The decrease in PV on Day 12 reflects the conversion of hydroperoxides into secondary oxidation products such as aldehydes, ketones, and alcohols, which produce a rancid odour and render the oils unusable. Rancidity developed earlier in camelina seed oil, indicating that the ketocarotenoid-rich oil has greater oxidative stability. While astaxanthin initially protects against oxidation, it eventually begins to oxidize as well. The results show that oleogel formation further protects the oils, with the stability of ketocarotenoid-rich oil matching that of the camelina seed oleogel. Converting ketocarotenoid-rich camelina oil into oleogel significantly boosted its stability, making it ideal for food applications. In the accelerated storage test, the PV and *p*-anisidine values of the astaxanthin-rich oleogel remained unchanged for the first 3 days, with only a slight PV increase until Day 9. While *p*-anisidine values rose significantly in camelina seed oil and its oleogel, no significant increase occurred in the astaxanthin-rich oil or its

oleogel, demonstrating the antioxidant effectiveness of astaxanthin and related ketocarotenoids as well as the added protective effect of the oleogel.

Discussion

Metabolic engineering of astaxanthin production in plants has emerged as a promising approach to meet the demands of the sustainable food, feed and cosmetic industries (Farré et al., 2016; Fujisawa et al., 2009; Ha et al., 2019; He et al., 2022; Liu et al., 2021; Lu et al., 2017; Park et al., 2017; Wang et al., 2021; Zhu et al., 2018). In this report, we compared the effectiveness of two astaxanthin biosynthetic pathways: one derived from *Adonis* and the other from bacteria, by transiently expressing these pathways in *N. benthamiana* leaves. Leaves expressing the *Adonis* gene set or a combination of *Adonis* and bacterial genes produced higher levels of astaxanthin and fewer ketocarotenoid intermediates compared to leaves expressing only the bacterial genes, suggesting that the plant-derived pathway may be more efficient under the conditions tested. Furthermore, the introduction of the *Adonis*-derived astaxanthin biosynthetic pathway, including the *CBFD2* and *HBFD1* genes along with the *ZmPSY* gene, resulted in the production of ketocarotenoids (~136 µg/g DW), including astaxanthin (~47 µg/g DW), in camelina seeds. These camelina seeds showed minimal accumulation of β-carotene. In contrast, previous studies using the bacterial pathway in soybean reported high levels of β-carotene and relatively lower levels of ketocarotenoids (Park et al., 2017; Pierce et al., 2015). The nearly complete conversion of β-carotene to ketocarotenoids in our study is advantageous for the production of natural red pigments for food and aquaculture applications (e.g. as colouring). Overall, our results suggest that *Adonis* genes provide higher yields and purer ketocarotenoid esters in an oilseed host compared to bacterial genes. Additionally, our findings highlight the utility of the transient *N. benthamiana* expression system for characterizing ketocarotenoid biosynthetic genes.

While metabolic engineering of astaxanthin production has been reported in several plant organs, including rapeseed, tomato, tobacco, maize, lettuce, carrot, rice and soybean, crop seed platforms are particularly attractive due to their ability to be grown on large land areas with modest inputs, ease of harvest, and potential for long-term storage prior to processing. Efforts to engineer astaxanthin production in crop seeds have focused on starch-rich cereal grains and oilseeds. Among these, oilseeds likely have greater commercial potential as an astaxanthin feedstock because astaxanthin can be co-extracted with the oil and can be further enriched through distillation. Recent studies have explored the production of astaxanthin in both cereal and oilseed crops. Notably, two cereal crops have been engineered for astaxanthin production in their endosperm (Farré et al., 2016; Ha et al., 2019; Liu et al., 2021; Zhu et al., 2018). The rice variety aSTARice, which expresses the *PSY*, *crtI*, *BCH* and *BKT* genes, accumulates astaxanthin up to 16.2 µg/g DW in the endosperm, accounting for approximately 74% of the total carotenoids, and also contains 3.3 µg/g DW intermediates such as adonixanthin and canthaxanthin (Zhu et al., 2018). Similarly, Ha et al. (2019) reported the production of 1.05 µg/g DW astaxanthin and 0.32 µg/g DW adonixanthin in rice endosperm using a polycistronic transgene approach. In maize, the particle bombardment method expressing *PSY1*, *BKT*, *crtZ*, and RNAi-*LYCE* led to the accumulation of 15.67 µg/g DW astaxanthin and 8.3 µg/g DW of intermediates

(Farré et al., 2016), while Liu et al. (2021) reported that maize expressing *PSY1*, *crtI*, *BKT*, and *crtZ* genes achieved the highest astaxanthin levels, approximately 112 µg/g DW. Although these results are promising, the accumulation of total ketocarotenoids, including astaxanthin and its intermediates, in cereal crops is relatively modest compared to those in oilseed crops. In oilseed crops, three species have been developed for astaxanthin production in seeds. Transgenic rapeseed expressing *crtW* and *crtZ*, along with β-carotene supply genes (e.g. *crtB* and *crtY*), accumulated 0.6 µg/g FW of astaxanthin and 190 µg/g FW of intermediates (Fujisawa et al., 2009). Transgenic soybean expressing *PSY1*, *crtW* and *crtZ* genes accumulated 25 µg/g DW astaxanthin and 55 µg/g DW intermediates (Park et al., 2017). Camelina, engineered to express the *Orange* (*Or*) gene, *crtB*, *CHYB* and *BKT* genes, produced 42.7 µg/g DW astaxanthin and 114.6 µg/g DW intermediates (He et al., 2022). Notably, oilseed crops expressing bacteria-derived astaxanthin genes, combined with β-carotene supply genes, exhibit at least a 10-fold higher accumulation of β-carotene compared to astaxanthin, with significant increases in intermediates (more than a fourfold increase compared to astaxanthin). Our engineered camelina seeds, which express plant-derived astaxanthin genes and the β-carotene supply enzyme (*PSY*), contain only trace amounts of β-carotene but accumulate ketocarotenoid intermediates at levels approximately 1.5-fold those of astaxanthin (47.1 µg/g DW astaxanthin and 71.9 µg/g DW intermediates; Figure 5). These findings suggest that optimizing both the β-carotene supply and the selection of appropriate astaxanthin biosynthetic enzymes is an effective strategy for enhancing the conversion of β-carotene to astaxanthin.

Engineering the accumulation of astaxanthin in camelina seeds in our studies resulted in reduced total oil and tocopherol concentrations, as well as delayed seed germination. Geranylgeranyl pyrophosphate (GGPP), a precursor from the upstream methylerythritol (MEP) pathway, is integral to the biosynthesis of both tocopherols and carotenoids (DellaPenna and Pogson, 2006). Accordingly, the decrease in tocopherol content observed in pASTA seeds, alongside the increased carotenoid levels, is consistent with the expected effects of manipulating GGPP. The mechanism behind the delayed germination in pASTA seeds remains unclear. Carotenoids, precursors for ABA synthesis, suggest that changes in carotenoid metabolism could disrupt ABA production, affecting seed dormancy and germination (Ali et al., 2022; Sybilska and Daszkowska-Golec, 2023). Previous studies have shown that carotenoid-accumulating Arabidopsis lines expressing *PSY* genes exhibit delayed germination, possibly due to elevated ABA levels (Lindgren et al., 2003). Conversely, improved germination in transgenic seeds expressing *PSY* and *Or* genes was observed when the ABA biosynthetic pathway was disrupted by knocking out β-carotene hydroxylase 2 (Sun et al., 2021). However, our study detected no significant change in ABA content in pASTA seeds compared to the wild type, suggesting that the delayed germination observed in pASTA seeds may be independent of ABA.

Notably, previous studies have shown that even moderate carotenoid overaccumulation can negatively affect germination, likely by interfering with plastid metabolism or hormonal homeostasis (Allorent et al., 2014; Lindgren et al., 2003). Therefore, the delayed germination observed in pASTA seeds may be at least partially attributable to the accumulation of ketocarotenoids. If this is the case, sequestration of excess carotenoids, for example through esterification of astaxanthin,

may help alleviate the adverse effects on seed germination. Additionally, we observed that the cotyledons of germinating pASTA seeds display altered pigmentation compared to wild-type. Similar to previous reports in camelina expressing high levels of polyhydroxybutyrate (PHB), where cotyledon chlorosis and variegation were linked to excessive metabolite accumulation (Malik *et al.*, 2014), the altered cotyledon colour in pASTA seedlings may reflect plastid dysfunction caused by the accumulation of non-native ketocarotenoids. This could contribute to the delayed seed germination phenotype, potentially through impaired chloroplast development or altered plastid metabolism.

As an additional aspect of our research, we showed the utility of our ketocarotenoid-rich oil for novel food science applications in oleogels. Oleogels are versatile, semi-solid gels created by immobilizing liquid oils within a three-dimensional network of structuring agents, forming a gel-like structure without the need for hydrogenation or solid fats (Puşcaş *et al.*, 2020). Designed to mimic the texture and functionality of solid fats such as butter and margarine, oleogels provide similar properties, including spreadability and stability, but without the associated trans fats (Puşcaş *et al.*, 2020). Oleogels are gaining popularity in food applications due to their ability to reduce saturated and trans fats in products like spreads, baked goods and chocolates, offering a healthier alternative to traditional fats (Demirci *et al.*, 2020). Beyond food, they are also used in pharmaceuticals and cosmetics for their biocompatibility and controlled release potential, as well as in biodegradable lubricants as a sustainable alternative (Martinez *et al.*, 2019). In this study, oleogels were used to convert astaxanthin-enriched camelina seed oil into a stable, semi-solid fat structure with an enhanced shelf life. Astaxanthin, a powerful antioxidant, not only boosts the oxidative stability of camelina oil but also offers numerous health benefits, including anti-inflammatory effects and cardiovascular support (Cao *et al.*, 2023; Sánchez-Camargo *et al.*, 2012; Yuan *et al.*, 2011). In this study, sorghum grain wax was used as a natural, plant-based oleogelator due to its physicochemical similarity to carnauba wax and its proven ability to form stable oleogels with desirable properties (Liu *et al.*, 2020; Sperotto *et al.*, 2022). Figure 7 demonstrates how astaxanthin and other ketocarotenoids significantly reduce the formation of primary and secondary oxidation products in camelina oil and oleogels, extending stability compared to untreated oils. Currently, over 95% of astaxanthin used in aquaculture is synthetic, but natural sources are in demand, often extracted from microalgae (Sánchez-Camargo *et al.*, 2012). Incorporating natural astaxanthin into edible oils is a promising, cost-effective way to add functional value to commodity oils. However, astaxanthin is sensitive to light and oxygen, which can degrade it during storage. Converting astaxanthin-rich camelina oil into an oleogel protects both the astaxanthin and the oil itself, creating a fat-mimicking, semi-solid structure with improved stability and nutritional value, making these oleogels excellent candidates for food and nutraceutical applications.

In conclusion, we applied the ketocarotenoid biosynthetic pathway from *A. aestivalis* into camelina and detected 136 µg/g DW of ketocarotenoids and 47 µg/g DW of astaxanthin production in seeds. We also showed that astaxanthin-rich oil/oleogel contains a lower peroxidase value and higher oxidative stability compared to camelina oil/oleogel. Our study demonstrated the potential of the plant-derived astaxanthin biosynthetic pathway for astaxanthin production in oilseed crops and provided evidence for the feasibility of using astaxanthin as an antioxidant additive in solid fats.

Experimental procedures

Plant materials and field growth condition

Camelina sativa (L. cv. Suneson) and *N. benthamiana* were germinated in soil and grown under greenhouse conditions with a 14-h day length (24–26 °C) and an 8-h dark (18–20 °C) with natural and supplemental lighting at 400–500 µmole/m²/s. Transgenic camelina and wild-type plants were grown in the field at Eastern Nebraska Research, Extension and Education Center (ENREEC) in Mead, Nebraska, US in 2019 and 2020 growing seasons (under USDA APLI permit), and at Rothamsted Research (RRes) in Harpenden, Hertfordshire, UK from 2016 to 2018 and in 2020 growing seasons (under Defra consents 16/R8/01 and 18/R8/01). For the field experiments, each biological replicate consisted of an independent row of plants that was harvested separately within the same treatment group. These replicate rows were spatially separated within the field to account for potential microenvironmental variation. The harvested seeds were dried at room temperature for over a week before being used in all experiments.

Vector construction and plant transformation

For transient expression in *N. benthamiana* leaves, two binary vector constructs were designed to express *CBFD2* and *HBFD1* or *TP-crtW* and *TP-crtZ* genes under the control of the CaMV 35S promoter and the CaMV 35S 3' untranslated region (UTR). The GoldenBraid 2.0-based modular DNA assembly system was used for multigene assembly (Sarrion-Perdigones *et al.*, 2013); p35S-ASTA (*CBFD2* + *HBFD1*), p35S-crtWZ (*TP-crtW* + *TP-crtZ*), p35S-COMBI (*CBFD2* + *HBFD1* + *TP-crtW* + *TP-crtZ*). The agrobacterium (strain GV3101) harbouring p35S-ASTA, p35S-crtWZ or p35S-COMBI was incubated in infiltration buffer (10 mM MES, pH 5.8; 10 mM MgCl₂; 500 µM acetosyringone) for 1 h. Agrobacterium cells were infiltrated using a disposable, needleless syringe. *N. benthamiana* leaves were collected 5 days after infiltration (5 DAI) and used for thin layer chromatograph (TLC) and high-performance liquid chromatograph (HPLC) analysis.

The carotenoid β -ring 4-dehydrogenase 2 (*CBFD2*; AY644759.1 and AY644758.1), carotenoid 4-hydroxy- β -ring 4-dehydrogenase 1 (*HBFD1*; DQ902555.1), β -carotene ketolase (*crtW*; QVQ68840.1), β -carotene hydroxylase (*crtZ*; WP_183216731.1) and phytoene synthase (*PSY*; NM_001114652.2) cDNAs were used. The transit peptide (TP; 58 amino acid residues) from the small subunit of the Rubisco complex (At1g67090) was fused to the coding sequences of *crtW* and *crtZ* for plastid targeting (*TP-crtW* and *TP-crtZ*, respectively). Each cDNA was synthesized with codon optimization for dicotyledon plants. The synthesized DNA fragment was tagged with restriction enzyme sites *EcoRI* (5') and *XhoI* (3') and subcloned into the binary vector pBinGlyBar (Nguyen *et al.*, 2015), which contains a seed-specific glycinin promoter and glycinin terminator, and two cassettes digested with *AvrII* and *SpeI* were added to the pBinGlyBar binary vector using the *SpeI* restriction enzyme in the multiple cloning sites region. Camelina was transformed with the designed binary vector by Agrobacterium (GV3101 strain)-mediated floral dip method (Lu and Kang, 2008), and the transgenic line (ASTA) was selected by the red colour of astaxanthin-producing seeds. Approximately 20 selected T₁ seeds representing independent transgenic events were propagated under greenhouse conditions. Concentrations of astaxanthin and other ketocarotenoids were measured in seeds harvested from

these lines. The line with the highest concentrations of astaxanthin and other ketocarotenoids was selected for advancement to subsequent generations to assess homozygosity. The line used for in-depth characterization and field plantings was from the >T₅ generation.

Extraction and TLC analysis of carotenoids

Fifty milligrams of camelina seeds was prepared for the extraction of carotenoids. The camelina seeds or *N. benthamiana* leaves were ground into a fine powder using a homogenizer with extraction solvent (methanol:dichloromethane, 75:25, v/v). One volume of distilled water was added to the samples and carotenoids were subsequently extracted with chloroform. The organic phase was transferred and evaporated under nitrogen gas. The residue was resuspended in acetone. Carotenoids and neutral lipids (triacylglycerol and wax ester) from extracts were separated by first performing TLC with a mobile phase (heptane: ethyl ether:acetic acid; 80:20:0.1, v/v/v) and subsequently separated by second TLC with mobile phase (toluene:acetone; 80:20, v/v). Ketocarotenoids and astaxanthin were scraped from the TLC plate and dissolved in the extraction solvent. Extracted carotenoids were used for the following reactions: (1) Trimethylsilyl (TMS) derivatives were formed by adding equal volumes of pyridine and N,O-Bis (trimethylsilyl) acetamide. The TMS derivatives were concentrated under nitrogen gas and dissolved in acetone. TMS derivatives were separated by TLC with mobile phase (toluene:acetone; 80:20, v/v). (2) Reduced ketocarotenoids were formed by adding a sodium borohydride solution. The reactants were extracted using heptane. The extracts were concentrated under nitrogen gas and dissolved in acetone. Reduced ketocarotenoids were separated by TLC with a mobile phase (toluene:acetone; 50:50, v/v).

HPLC analysis of carotenoids and tocopherols

Carotenoid extracts, along with β -apo-8'-carotenal and 5,7-dimethyltolcol as internal standards (1 μ g each) for carotenoids and tocopherols, were dissolved in a solvent mixture (methanol: dichloromethane, 9:1, v/v) and injected into an HPLC system (Agilent 1200 Series) equipped with diode array detection (DAD) and fluorescence detection (FLD). Carotenoids were separated using C18 reverse-phase columns (Agilent Eclipse XDB-C18; 5 μ m, 4.6 \times 150 mm) with the following mobile phase conditions: the mobile phase consists of water (A) and methanol: methyl *tert*-butyl ether (8:2, v/v) (B). The gradient was 10% A: 90% B for 10 min with a flow rate of 1.0 mL/min, stepped to 10% A: 90% B for 5 min with a flow rate of 1.5 mL/min, and then to 100% B for 25 min with a flow rate of 1.5 mL/min. The column temperature was maintained at 30 °C and carotenoids and tocopherols were detected by DAD at 455 nm and by FLD (excitation at 292 nm; emission at 330 nm), respectively.

Seed oil analysis

The crushed camelina seeds (20 mg), glyceryl triheptadecanoate (100 μ g; as an internal standard) and 2.5% H₂SO₄ (in methanol) were heated for 30 min to generate fatty acid methyl esters (FAMES). FAMES were extracted with heptane and directly examined by gas chromatography (GC)-flame ionization detector (FID) (Agilent 7890A) equipped with a HP-INNOWAX column (length 30 m, diameter 0.25 mm, film 0.25 μ m; J&W 19091N-133I). The GC conditions were as follows: Inlet temperature: 275 °C. GC oven initial temperature: 90 °C, Hold Time: 1 min. Rate 30 °C/min to 235 °C, Hold Time: 5 min. FID detector

temperature: 275 °C. The peak area at each retention time was calculated based on the concentration of the internal standard and its corresponding peak area.

ABA analysis

The developing camelina seeds were ground into a fine powder using liquid nitrogen and dissolved in a hormone extraction solvent (isopropanol:water:concentrated HCl, 2:1:0.002, v/v/v) with Δ 6-ABA as an internal standard. Hormones were extracted and washed with dichloromethane. The organic phase was transferred to a new tube and concentrated under nitrogen gas. The hormones were quantified by HPLC-mass spectrometry as previously described (Pan et al., 2010).

Oleogel formation

Oleogels were prepared according to Liu et al. (2020). Briefly, sorghum wax was mixed with both astaxanthin-rich camelina seed oil and camelina seed oil (control) at a 6% (w/w) concentration to obtain a 50 g mixture. Sorghum wax was extracted using hexane at 60 °C for 1 h (Liu et al., 2020). The mixtures were then heated in an ultrasonic water bath (Fisher Scientific, Pennsylvania) at 85 °C for 15 min at a working power of 110 W and a frequency of 40 kHz. Samples were cooled in an ice bath to solidify the mixtures to obtain the oleogels. The oleogel samples were stored at 4 °C until analysed. Camelina seed oils were obtained for these experiments by use of a cold screw press (AgOilPress).

Determination of the oxidative stability

The oxidative stability of the oleogels was determined using an accelerated oxidation test by monitoring the formation of primary and secondary oxidation products (Liu et al., 2020). One gram of oleogel samples and the controls (camelina seed oil and astaxanthin-rich camelina seed oil) were stored in open-lid vials (1.5 mL) at 40 °C in an oven. Vials were withdrawn every 3 days to assess the primary and secondary oxidation products. Details of oxidative stability studies are provided in Appendix S1.

Acknowledgements

We thank Pat Tenopir (University of Nebraska-Lincoln Plant Biotechnology Field Facility) for camelina field management. JAN thanks the Nutrition Analytical Services unit of the Institute of Aquaculture, University of Stirling for their help in carotenoid analysis. We thank Professor Paul Fraser and lab (Royal Holloway, University of London) for consultation on ketocarotenoid compositional analyses. We thank undergraduate students Gannon Cole, Bernadette Traina, Shane Rice and Nikole Salas for their contributions to the research as part of the USDA-NIFA Research and Extension Experiences for Undergraduates program "Expanding Opportunities in Agricultural Sciences: Crop to Food Innovation". We thank Loren Isom, Industrial Agriculture Products Center, University of Nebraska-Lincoln, for camelina seed pressing.

Author contributions

HJK, TN, JAN and EBC conceived the study. HK, KP, OC, JAN and EBC wrote the manuscript. HK and TN generated expression constructs and transgenic camelina plants. HK conducted the transient expression assay in *N. benthamiana*. TJN and EBC managed the field evaluations in Nebraska. HK conducted lipid,

carotenoids and tocopherols analyses. REC conducted ABA analysis. LH and JAN managed the field evaluations in the UK. LH conducted lipid and carotenoids analyses. LL and OC conducted the oxidative stability test on seed oil. RPH conducted the TAG profiling. EBC provided overall supervision for the project.

Conflict of interest

The authors declare no competing financial interests.

Funding

This work was funded by United States Department of Agriculture National Institute of Food and Agriculture grant no. 2021-67013-33899 and the Nebraska Soybean Board to EBC. Food application research was funded in part by a NSF Global Centers grant #2435264 to OC and EBC. Undergraduate student participation was supported by United States Department of Agriculture National Institute of Food and Agriculture grant no. 2022-67037-36616 to EBC and OC. JAN and LH were partially supported by funding from BBSRC (UK) grant # BBS/E/RH/230002B and BBS/E/C/00010420.

Data availability statement

The data that support the findings of this study are available on request from the corresponding author. The data are not publicly available due to privacy or ethical restrictions.

References

- Alcaino, J., Fuentealba, M., Cabrera, R., Baeza, M. and Cifuentes, V. (2012) Modeling the interfacial interactions between CrtS and CrtR from *Xanthophyllomyces dendrorhous*, a P450 system involved in astaxanthin production. *J. Agric. Food Chem.* **60**, 8640–8647.
- Ali, F., Qanmber, G., Li, F. and Wang, Z. (2022) Updated role of ABA in seed maturation, dormancy, and germination. *J. Adv. Res.* **35**, 199–214.
- Allorent, G., Osorio, S., Ly Vu, J., Falconet, D., Jouhet, J., Kuntz, M., Fernie, A.R. et al. (2014) Adjustments of embryonic photosynthetic activity modulate seed fitness in *Arabidopsis thaliana*. *New Phytologist* **205**(2), 707–719.
- Allen, Q.M., Febres, V.J., Rathinasabapathi, B. and Chaparro, J.X. (2022) Engineering a plant-derived astaxanthin synthetic pathway into *Nicotiana benthamiana*. *Front. Plant Sci.* **12**, 831785.
- Álvarez, V., Rodríguez-Sáiz, M., de la Fuente, J.L., Gudiña, E.J., Godio, R.P., Martín, J.F. and Barredo, J.L. (2006) The *crtS* gene of *Xanthophyllomyces dendrorhous* encodes a novel cytochrome-P450 hydroxylase involved in the conversion of β -carotene into astaxanthin and other xanthophylls. *Fungal Genet. Biol.* **43**, 261–272.
- Cao, Y., Yang, L., Qiao, X., Xue, C. and Xu, J. (2023) Dietary astaxanthin: an excellent carotenoid with multiple health benefits. *Crit. Rev. Food Sci. Nutr.* **63**, 3019–3045.
- Cunningham, F.X., Jr. and Gantt, E. (2011) Elucidation of the pathway to astaxanthin in the flowers of *Adonis aestivalis*. *Plant Cell*, **23**, 3055–3069.
- Debnath, T., Bandyopadhyay, T.K., Vanitha, K., Bobby, M.N., Tiwari, O.N., Bhunia, B. and Muthuraj, M. (2024) Astaxanthin from microalgae: a review on structure, biosynthesis, production strategies and application. *Food Res. Int.* **176**, 113841.
- DellaPenna, D. and Pogson, B.J. (2006) Vitamin synthesis in plants: tocopherols and carotenoids. *Annu. Rev. Plant Biol.* **57**, 711–738.
- Demirci, M., Lee, C.C., Çavuş, M. and Çağlar, M.Y. (2020) Oleogels for food applications. In *Biopolymer-Based Formulations: biomedical and Food Applications* (Pal, K., Banerjee, I., Sarkar, P., Kim, D., Deng, W.-P., Dubey, N.K. and Majumder, K., eds), pp. 781–811. Amsterdam, The Netherlands: Elsevier Inc.
- Elbahnaswy, S. and Elshopakey, G.E. (2024) Recent progress in practical applications of a potential carotenoid astaxanthin in aquaculture industry: a review. *Fish Physiol. Biochem.* **50**, 97–126.
- Farré, G., Perez-Fons, L., Decourcelle, M., Breitenbach, J., Hem, S., Zhu, C., Capell, T. et al. (2016) Metabolic engineering of astaxanthin biosynthesis in maize endosperm and characterization of a prototype high oil hybrid. *Transgenic Res.* **25**, 477–489.
- Fernández-González, B., Sandmann, G. and Vioque, A. (1997) A new type of asymmetrically acting β -carotene ketolase is required for the synthesis of echinenone in the cyanobacterium *Synechocystis* sp. PCC 6803. *J. Biol. Chem.* **272**, 9728–9733.
- Frankel, E.N. (1984) Lipid oxidation: mechanisms, products and biological significance. *J. Am. Oil Chem. Soc.* **61**, 1908–1917.
- Fujisawa, M., Takita, E., Harada, H., Sakurai, N., Suzuki, H., Ohyama, K., Shibata, D. et al. (2009) Pathway engineering of *Brassica napus* seeds using multiple key enzyme genes involved in ketocarotenoid formation. *J. Exp. Bot.* **60**, 1319–1332.
- Grand View Research. (2024) *Astaxanthin market size & share report, 2030*. <https://www.grandviewresearch.com/industry-analysis/global-astaxanthin-market>
- Ha, S.-H., Kim, J.K., Jeong, Y.S., You, M.-K., Lim, S.-H. and Kim, J.-K. (2019) Stepwise pathway engineering to the biosynthesis of zeaxanthin, astaxanthin and capsanthin in rice endosperm. *Metab. Eng.* **52**, 178–189.
- He, M.-X., Wang, J.-L., Lin, Y.-Y., Huang, J.-C., Liu, A.-Z. and Chen, F. (2022) Engineering an oilseed crop for hyper-accumulation of carotenoids in the seeds without using a traditional marker gene. *Plant Cell Rep.* **41**, 1751–1761.
- Huang, J.-C., Zhong, Y.-J., Liu, J., Sandmann, G. and Chen, F. (2013) Metabolic engineering of tomato for high-yield production of astaxanthin. *Metab. Eng.* **17**, 59–67.
- Iskandarov, U., Kim, H.J. and Cahoon, E.B. (2014) Camelina: an emerging oilseed platform for advanced biofuels and bio-based materials. In *Plants and BioEnergy. Advances in Plant Biology*, Vol. 4 (McCann, M., Buckeridge, M. and Carpita, N., eds), pp. 131–140. New York, USA: Springer.
- Kiczorowska, B., Samolińska, W., Andrejko, D., Kiczorowski, P., Antoszkiewicz, Z., Zajac, M., Winiarska-Mieczan, A. et al. (2019) Comparative analysis of selected bioactive components (fatty acids, tocopherols, xanthophyll, lycopene, phenols) and basic nutrients in raw and thermally processed camelina, sunflower, and flax seeds (*Camelina sativa* L. Crantz, *Helianthus L.*, and *Linum L.*). *J. Food Sci. Technol.* **56**, 4296–4310.
- Konda, A.R., Gelli, M., Pedersen, C., Cahoon, R.E., Zhang, C., Obata, T. and Cahoon, E.B. (2023) Vitamin E biofortification: maximizing oilseed tocotrienol and total vitamin E tocopherol production by use of metabolic bypass combinations. *Metab. Eng.* **79**, 66–77.
- Li, Y., Gong, F., Guo, S., Yu, W. and Liu, J. (2021) *Adonis amurensis* is a promising alternative to *Haematococcus* as a resource for natural esterified (3 S, 3' S)-Astaxanthin production. *Plants*, **10**, 1059.
- Lindgren, L.O., Stålberg, K.G. and Höglund, A.S. (2003) Seed-specific overexpression of an endogenous *Arabidopsis* phytoene synthase gene results in delayed germination and increased levels of carotenoids, chlorophyll, and abscisic acid. *Plant Physiol.* **132**, 779–785.
- Liu, L., Ramirez, I.S.A., Yang, J. and Ciftci, O.N. (2020) Evaluation of oil-gelling properties and crystallization behavior of sorghum wax in fish oil. *Food Chem.* **309**, 125567.
- Liu, X., Ma, X., Wang, H., Li, S., Yang, W., Nugroho, R.D., Luo, L. et al. (2021) Metabolic engineering of astaxanthin-rich maize and its use in the production of biofortified eggs. *Plant Biotechnol. J.* **19**, 1812–1823.
- Lu, C. and Kang, J. (2008) Generation of transgenic plants of a potential oilseed crop *Camelina sativa* by *Agrobacterium*-mediated transformation. *Plant Cell Rep.* **27**, 273–278.
- Lu, Y., Stegemann, S., Agrawal, S., Karcher, D., Ruf, S. and Bock, R. (2017) Horizontal transfer of a synthetic metabolic pathway between plant species. *Curr. Biol.* **27**, 3034–3041.e3.
- Malik, M.R., Yang, W., Patterson, N., Tang, J., Wellingshoff, R.L., Preuss, M.L., Burkitt, C. et al. (2014) Production of high levels of poly-3-hydroxybutyrate in plastids of *Camelina sativa* seeds. *Plant Biotechnology Journal* **13**(5), 675–688.
- Malik, M.R., Tang, J., Sharma, N., Burkitt, C., Ji, Y., Mykytyshyn, M., Bohmert-Tatartev, K. et al. (2018) *Camelina sativa*, an oilseed at the nexus between model system and commercial crop. *Plant Cell Rep.* **37**, 1367–1381.

- Maoka, T. (2020) A new carotenoid, 5, 6-dihydrocrustaxanthin, from prawns and the distribution of yellow xanthophylls in shrimps. *Biochem. Syst. Ecol.* **92**, 104083.
- Maoka, T., Etoh, T., Kishimoto, S. and Sakata, S. (2011) Carotenoids and their fatty acid esters in the petals of *Adonis aestivalis*. *J. Oleo Sci.* **60**, 47–52.
- Martinez, R.M., Rosado, C., Velasco, M.V.R., Lannes, S.C.D.S. and Baby, A.R. (2019) Main features and applications of organogels in cosmetics. *Int. J. Cosmet. Sci.* **41**, 109–117.
- Martins, A.J., Vicente, A.A., Pastrana, L.M. and Cerqueira, M.A. (2020) Oleogels for development of health-promoting food products. *Food Sci. Human Wellness*, **9**, 31–39.
- Meléndez-Martínez, A.J., Britton, G., Vicario, I.M. and Heredia, F.J. (2007) Relationship between the colour and the chemical structure of carotenoid pigments. *Food Chem.* **101**, 1145–1150.
- Miki, W. (1991) Biological functions and activities of animal carotenoids. *Pure Appl. Chem.* **63**, 141–146.
- Mulders, K.J., Weesepeel, Y., Bodenes, P., Lamers, P.P., Vincken, J.-P., Martens, D.E., Gruppen, H. et al. (2015) Nitrogen-depleted *Chlorella zofingiensis* produces astaxanthin, ketolutein and their fatty acid esters: a carotenoid metabolism study. *J. Appl. Phycol.* **27**, 125–140.
- Nakano, T. (2020) Stress in fish and application of carotenoid for aquafeed as an antistress supplement. In *Encyclopedia of Marine Biotechnology* (Kim, S.-K., ed), pp. 2999–3019. Hoboken, USA: John Wiley & Sons Publications.
- Napier, J.A. and Betancor, M.B. (2023) Engineering plant-based feedstocks for sustainable aquaculture. *Curr. Opin. Plant Biol.* **71**, 102323.
- Napier, J.A. and Sayanova, O. (2020) Nutritional enhancement in plants—green and greener. *Curr. Opin. Biotechnol.* **61**, 122–127.
- Nguyen, H.T., Park, H., Koster, K.L., Cahoon, R.E., Nguyen, H.T.M., Shanklin, J., Clemente, T.E. et al. (2015) Redirection of metabolic flux for high levels of omega-7 monounsaturated fatty acid accumulation in camelina seeds. *Plant Biotechnol. J.* **13**, 38–50.
- O'Connor, I. and O'Brien, N. (1998) Modulation of UVA light-induced oxidative stress by β -carotene, lutein and astaxanthin in cultured fibroblasts. *J. Dermatol. Sci.* **16**, 226–230.
- Ojima, K., Breitenbach, J., Visser, H., Setoguchi, Y., Tabata, K., Hoshino, T., van den Berg, J. et al. (2006) Cloning of the astaxanthin synthase gene from *Xanthophyllomyces dendrorhous* (*Phaffia rhodozyma*) and its assignment as a β -carotene 3-hydroxylase/4-ketolase. *Mol. Gen. Genomics*, **275**, 148–158.
- Pan, X., Welti, R. and Wang, X. (2010) Quantitative analysis of major plant hormones in crude plant extracts by high-performance liquid chromatography–mass spectrometry. *Nat. Protoc.* **5**, 986–992.
- Park, H., Weier, S., Razvi, F., Peña, P.A., Sims, N.A., Lowell, J., Hungate, C. et al. (2017) Towards the development of a sustainable soya bean-based feedstock for aquaculture. *Plant Biotechnol. J.* **15**, 227–236.
- Pierce, E.C., LaFayette, P.R., Ortega, M.A., Joyce, B.L., Kopsell, D.A. and Parrott, W.A. (2015) Ketocarotenoid production in soybean seeds through metabolic engineering. *PLoS One*, **10**, e0138196.
- Puşcaş, A., Mureşan, V., Socăci, C. and Muste, S. (2020) Oleogels in food: a review of current and potential applications. *Foods*, **9**, 70.
- Renström, B., Berge, H. and Liaaen-Jensen, S. (1981) Esterified, optical pure (3S, 3'S)-astaxanthin from flowers of *Adonis annua*. *Biochem. Syst. Ecol.* **9**, 249–250.
- Sánchez-Camargo, A.P., Meireles, M.Â.A., Ferreira, A.L., Saito, E. and Cabral, F.A. (2012) Extraction of ω -3 fatty acids and astaxanthin from Brazilian redspotted shrimp waste using supercritical CO₂/ ethanol mixtures. *J. Supercrit. Fluids*, **61**, 71–77.
- Santocono, M., Zurria, M., Berrettini, M., Fedeli, D. and Falcioni, G. (2006) Influence of astaxanthin, zeaxanthin and lutein on DNA damage and repair in UVA-irradiated cells. *J. Photochem. Photobiol. B Biol.* **85**, 205–215.
- Sarrion-Perdigones, A., Vazquez-Vilar, M., Palací, J., Castelijns, B., Forment, J., Ziaresolo, P., Blanca, J. et al. (2013) GoldenBraid 2.0: a comprehensive DNA assembly framework for plant synthetic biology. *Plant Physiol.* **162**, 1618–1631.
- Seybold, A. and Goodwin, T.W. (1959) Occurrence of astaxanthin in the flower petals of *Adonis annua* L. *Nature*, **184**, 1714–1715.
- Sperotto, F., Yang, J., Isom, L., Weller, C. and Ciftci, O.N. (2022) Supercritical carbon dioxide extraction, purification, and characterization of wax from sorghum and sorghum by-products as an alternative natural wax. *J. Am. Oil Chem. Soc.* **99**, 1–9.
- Suganuma, K., Nakajima, H., Ohtsuki, M. and Imokawa, G. (2010) Astaxanthin attenuates the UVA-induced up-regulation of matrix-metalloproteinase-1 and skin fibroblast elastase in human dermal fibroblasts. *J. Dermatol. Sci.* **58**, 136–142.
- Sun, T., Zhu, Q., Wei, Z., Owens, L.A., Fish, T., Kim, H., Thannhauser, T.W. et al. (2021) Multi-strategy engineering greatly enhances provitamin A carotenoid accumulation and stability in *Arabidopsis* seeds. *Abiotech*, **2**, 191–214.
- Sybilka, E. and Daszkowska-Golec, A. (2023) Alternative splicing in ABA signaling during seed germination. *Front. Plant Sci.* **14**, 1144990.
- Ukibe, K., Hashida, K., Yoshida, N. and Takagi, H. (2009) Metabolic engineering of *Saccharomyces cerevisiae* for astaxanthin production and oxidative stress tolerance. *Appl. Environ. Microbiol.* **75**, 7205–7211.
- Wang, J.L., Tan, S.L., He, M.X., Huang, W. and Huang, J.C. (2021) Ketocarotenoids accumulation in the leaves of engineered *Brassica napus* restricts photosynthetic efficiency and plant growth. *Environ. Exp. Bot.* **186**, 104461.
- Xi, J., Rossi, L., Lin, X. and Xie, D.-Y. (2016) Overexpression of a synthetic insect-plant geranyl pyrophosphate synthase gene in *Camelina sativa* alters plant growth and terpene biosynthesis. *Planta*, **244**, 215–230.
- Yuan, J.-P. and Chen, F. (2000) Purification of trans-astaxanthin from a high-yielding astaxanthin ester-producing strain of the microalga *Haematococcus pluvialis*. *Food Chem.* **68**, 443–448.
- Yuan, L. and Li, R. (2020) Metabolic engineering a model oilseed *Camelina sativa* for the sustainable production of high-value designed oils. *Front. Plant Sci.* **11**, 11.
- Yuan, J.P., Peng, J., Yin, K. and Wang, J.H. (2011) Potential health-promoting effects of astaxanthin: a high-value carotenoid mostly from microalgae. *Mol. Nutr. Food Res.* **55**, 150–165.
- Zhu, Q., Zeng, D., Yu, S., Cui, C., Li, J., Li, H., Chen, J. et al. (2018) From golden rice to aSTARice: bioengineering astaxanthin biosynthesis in rice endosperm. *Mol. Plant*, **11**, 1440–1448.

Supporting information

Additional supporting information may be found online in the Supporting Information section at the end of the article.

Appendix S1 Experimental procedures.

Figure S1 Comparison of carotenoid ring modifications by enzymes from *Adonis*- and bacterial-derived pathways.

Figure S2 Generation of pASTA camelina.

Figure S3 Chlorophyll content and gene expression analysis related to chloroplast biogenesis in developing seeds and cotyledons.

Figure S4 HPLC analysis of total carotenoids extracted from seeds of pASTA grown in greenhouse.

Figure S5 TLC analysis ketocarotenoids extracted from seeds of pASTA grown in the greenhouse.

Figure S6 Agronomic traits analysis in seeds wild type and pASTA grown in the field at Rothamsted Research (RRes) in Harpenden, Hertfordshire, UK.

Table S1 Carotenoid profiles in *N. benthamiana* leaves transiently expressing *Adonis* genes (ASTA), bacterial genes (crtWZ) or their combination (COMBI) involved in astaxanthin biosynthesis.

Table S2 The fatty acid composition (mol %) in seed of wild type and pASTA grown in field at ENREEC, NE.

Table S3 Seed yield per plot from wild type and pASTA grown in field at Rothamsted Research (RRes) in Harpenden, Hertfordshire, UK.

Table S4 Primers used in this study.